RESTORATION ECOLOGY
The Journal of the Society for Ecological Restoration

SER SOCIETY FOR ECOLOGICAL RESTORATION

RESEARCH ARTICLE

Short-term effects of a large dam decommissioning on biofilm structure and functioning

Miren Atristain[1,2], Daniel von Schiller[3], Aitor Larrañaga[1], Arturo Elosegi[1]

Aging dams and the rising efforts to restore stream ecosystems are increasing the number of dam decommissioning programs. Although dam decommissioning aims at improving in-stream habitat, biodiversity, and ecosystem functioning in the long term, it might also cause ecological impacts in the short term due to the mobilization of the sediment accumulated in the reservoir. Benthic biofilm in particular can be impaired by episodes of high turbidity and scouring. We conducted a multiple before-after/control-impact experiment to assess the effects of the drawdown of a large dam (42 m tall), a first step to its decommissioning, on biofilm structure (biomass and chlorophyll-*a*) and functioning (metabolism, nutrient uptake, and organic matter breakdown). Our results show that the reservoir drawdown reduced the autotrophic biofilm biomass (chlorophyll-*a*) downstream from the dam, which in turn lowered metabolism. However, nitrogen and phosphorus uptake by the biofilm was not affected. Organic matter breakdown was slower below the dam than in nearby undammed reaches before and during drawdown. All drawdown effects quickly disappeared and reaches downstream from the dam approached values found in nearby undammed reaches. Thus, our results indicate that the effects of reservoir drawdown on stream biofilms exist but may be small and disappear rapidly.

Key words: before-after/control-impact, connectivity restoration, dam removal, mountain stream, reservoir drawdown, sediment release

Implications for Practice

- Stream biofilm responds rapidly to environmental changes and can thus be a good indicator for responses to ecological restoration projects such as dam decommissioning.
- Slow and progressive drawdown before completing dam decommissioning helps retaining sediment in the reservoir and thus reduces their potential downstream impacts.
- Monitoring dam decommissioning with robust experimental designs, such as before-after/control-impact, is essential to assess the recovery of the ecological integrity of the restored sites.

Introduction

The serial discontinuity concept theory (Ward & Stanford 1983) proposed that dams and associated reservoirs may drastically alter the river continuum. Indeed, research has shown that these infrastructures reduce the hydrogeomorphological variability of downstream reaches (Graf 2006), modifying the magnitude and the frequency of natural floods (Poff et al. 1997), and retaining most bedload and a substantial portion of the suspended load (Vericat & Batalla 2006; Tena et al. 2011). In addition, dams typically modify downstream thermal regimes (Hester & Doyle 2011) and alter water chemistry (Ellis & Jones 2013; Winton et al. 2019) and thus, biogeochemical cycling of multiple elements (Friedl & Wüest 2002; Maavara et al. 2020). These changes can affect both stream biodiversity (Wu et al. 2019) and ecosystem functioning (Aristi et al. 2014; Colas et al. 2016; von Schiller et al. 2016). Due to these environmental concerns, in combination with public safety and growing maintenance costs, as dams reach the end of their life expectancy, managers push toward dam decommissioning (Foley et al. 2017).

Decommissioning is a general term referring to the activities undertaken when a dam ceases to be functional, which ends with its total or partial removal (Perera et al. 2021). So far, almost 2,000 dams have been removed in the United States and in Europe, especially low weirs and small dams (Bellmore et al. 2017; Habel et al. 2020). Although dam removal is

Author contributions: AE, AL, DvS designed the experiment and acquired the funding; AE, DvS, MA performed the experiment and sampling campaigns; MA carried out laboratory analyses and calculations; MA, AL performed the statistical analyses; MA wrote the manuscript; all the authors reviewed the manuscript.

[1]Department of Plant Biology and Ecology, University of the Basque Country (UPV/EHU), Leioa 48940, Spain
[2]Address correspondence to M. Atristain, email miren.atristain@ehu.eus
[3]Department of Evolutionary Biology, Ecology and Environmental Sciences, University of Barcelona, Barcelona 08028, Spain

doi: 10.1111/rec.13779
Supporting information at:
http://onlinelibrary.wiley.com/doi/10.1111/rec.13779/suppinfo

nowadays considered a pivotal action for river restoration (Magilligan et al. 2016; Foley et al. 2017), the potential impacts on biological communities and ecosystem functioning caused by the mobilization of stored sediment, nutrients, and organic matter, as well as their recovery, are still poorly understood (Bellmore et al. 2019). This is especially true for large dams (i.e. higher than 15 m or 5–15 m in height and impounding more than 3 hm^3; Perera et al. 2021), which have been removed in much lower numbers and whose effects (e.g. hydrologic alterations) can differ dramatically from smaller dams, thus affecting the restoration success of dam removal (Bellmore et al. 2017; Foley et al. 2017). As river hydrogeomorphology, water chemistry, and the structure and functioning of biological communities are among the most affected by large dams, it is especially important to understand the effects of dam decommissioning on these variables to minimize the potential impacts and maximize the benefits of future decommissioning plans.

The stream biofilm constitutes a key agent in biogeochemical cycles and aquatic food webs (Besemer 2015; Battin et al. 2016), and can be severely affected by large dams (Ponsatí et al. 2015). Autotrophic biofilms tend to be favored by the hydrologic stability and reduced scouring caused by flow regulation, which promotes biomass and metabolism below large dams (Morley et al. 2008; Aristi et al. 2014; Smolar-Žvanut & Mikoš 2014; Ponsatí et al. 2015). On the contrary, the activity of heterotrophic biofilms has been reported to decrease below dams (Muehlbauer et al. 2009; Colas et al. 2016), suggesting that for these organisms the detrimental effects of altered thermal regimes and water chemistry override the effects of hydrological stability. These mentioned large dam effects on both autotrophic and heterotrophic biofilms are strongest just below the dam and decrease downstream as free-flowing tributaries join the main stem (Munn & Brusven 2004; Ellis & Jones 2013). Dam removal usually triggers the downstream movement of large amounts of sediment stored in the reservoir (Wilcox et al. 2014; Randle et al. 2015), which typically scours and reduces autotrophic biofilm biomass and activity (Francoeur & Biggs 2006; Izagirre et al. 2009; Bellmore et al. 2019). However, autotrophic biofilm could recover shortly after these sediments disperse, as it shows high resilience to physical disturbances (Steinman & McIntire 1990). Nevertheless, empirical information is limited to small dams or, in the case of large dams, to modeling exercises (Bellmore et al. 2019). Regarding organic matter breakdown, in which heterotrophic biofilm play a key role, information is limited to one publication on total leaf litter breakdown (Muehlbauer et al. 2009) that showed little response to dam removal. In any case, to our knowledge the effects of large dam decommissioning on stream biofilm functioning still need to be assessed.

Here, by means of a multiple before-after/control-impact (mBACI) design (Underwood 1994), we studied how the drawdown, a key step toward dam decommissioning, of a large (42 m tall) dam affected downstream biofilm structure and functioning. Specifically, we investigated changes in biofilm biomass and chlorophyll-*a* (Chl-*a*) as well as three benthic biofilm functions (i.e. metabolism, nutrient uptake, and microbial organic matter decomposition) before, during, and after the drawdown. Our general hypothesis was that reservoir drawdown would affect water physicochemical characteristics, which, in turn, would cause shifts in the studied functions. Therefore, we predicted that: (1) before drawdown, autotrophic biofilm metabolism and nutrient uptake would be higher downstream from the dam than in control reaches, because of hydrological stability, whereas microbial organic matter decomposition would be reduced due to degraded water quality; these effects would fade out downstream as the distance from the dam increases; (2) during reservoir drawdown, transport of suspended sediment would reduce the rates of the three studied functions, the highest effects occurring immediately downstream from the dam; and (3) after the drawdown, water characteristics downstream from the dam would quick approach those from control reaches, and because its high resilience, biofilm would too.

Methods

Study Site and Experimental Design

The Artikutza valley is a mountain headwater catchment located in the north of the Iberian Peninsula (Fig. 1). The hydrological network of Artikutza drains a 3,683 ha basin over schist, granite, and sandstone (Government of Navarre, IDENA). Average annual rainfall is 2,604 mm per year and the mean annual air temperature is 12.3°C (http://meteo.navarra.es/). The entire catchment has been strictly conserved since the municipality of San Sebastian acquired it in 1919 to ensure the supply of good quality drinking water. Therefore, Artikutza catchment is mostly covered by mature forests dominated by beech (*Fagus sylvatica* L.) and oak (*Quercus robur* L.) stands, dense autochthonous riparian vegetation with alder (*Alnus glutinosa* [L.] Gaertner) and ash (*Fraxinus excelsior* L.), some old exotic plantations of conifers and red oaks (*Quercus rubra* L.), and pasturelands on the highest terrain (Lozano & Latasa 2019).

The Enobieta Dam was designed with a water storage capacity of 2.5 hm^3, but geotechnic issues forced the municipality to reduce its capacity to 1.6 hm^3 when finished in 1947. The reservoir supplied water to San Sebastian for some decades, but metal concentrations (especially Fe and Mn) were often over legal thresholds for drinking water (EU Directive 2020/2184), and the town faced water shortages because of the small capacity of the modified dam. Therefore, in 1976, the Añarbe Dam (79 m tall and 43.8 hm^3 reservoir capacity) was built further downstream in the catchment. Afterward, the Enobieta Dam lost its strategic value, fell progressively in disuse, and had little or no maintenance, to the point of becoming a safety issue. For these reasons, the municipality decided in 2018 to decommission it. During 2018, the reservoir was slowly emptied by means of some old siphons and one of the two water-serving pipes that was still in operating condition. During this period (before), mainly surface water was released. When the water level in the reservoir was approximately 4 m high (December 2018), the bottom gate was repaired and opened, thus starting a period of sediment release (drawdown) with high turbidity episodes. This turbidity was mainly caused by the Enobieta Stream carving a

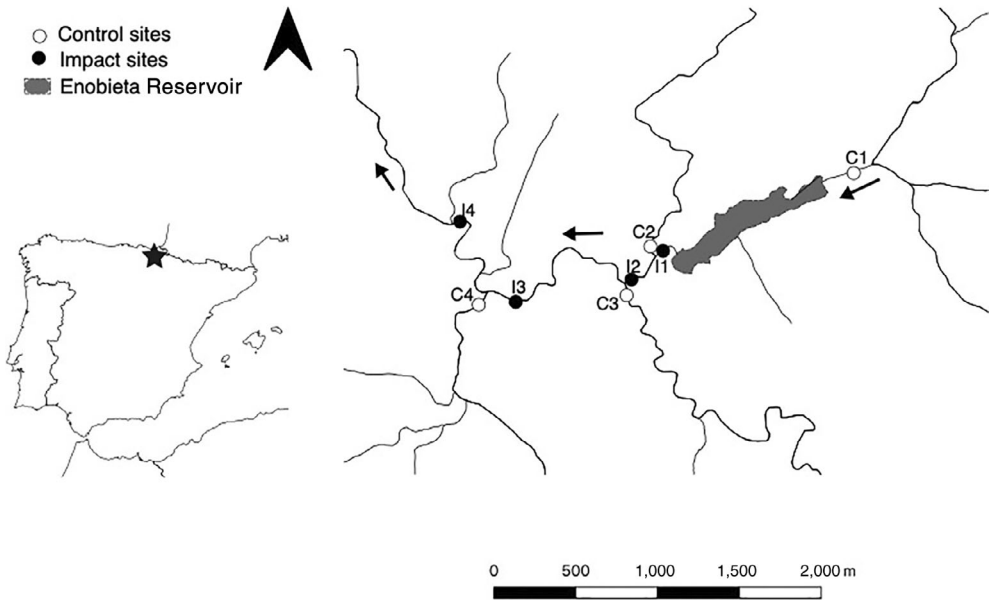

Figure 1. Study area showing the location of the eight study reaches (four control reaches [C1, C2, C3, and C4] and four impact reaches [I1, I2, I3, and I4]) in the Artikutza Valley (north Iberian Peninsula). The gray area indicates the area inundated by the Enobieta reservoir. Dark arrows indicate flow direction.

new channel across the sediment stored in the area closest to dam, whereas the sediment in the rest of the reservoir were mostly retained on site by the fast-growing vegetation (Elosegi et al. 2022). When the reservoir was empty, an older 3.5-m-tall weir emerged 200 m upstream from the large dam. The local managers demolished this weir in October 2019, and during the very rainy month of November 2019 the Enobieta Stream carved a new channel across the sediment retained by the weir, thus producing a last period of high turbidity. From this moment on, we considered the drawdown process to be finished and the after period to start. It is estimated that the total volume of sediment exported during the drawdown phase was 7,000 m^3, which corresponds to 8% of the sediment stored in the reservoir during 70 years of operation (Elosegi et al. 2022). Currently, the reservoir is empty, the bottom gate open, and the authorities are discussing whether to totally remove the dam or to open a 7-m-wide trench to remove the barrier effect. The final decision will depend exclusively on the expected damage and benefits each alternative can cause on the local biodiversity. Whatever the case, it has been estimated that any of these alternatives will mobilize considerably less sediment than those mobilized so far (Elosegi et al. 2022), and thus, will have smaller impacts on biofilm structure and functioning than the drawdown here reported.

We conducted a mBACI study in which we defined eight 100-m-long reaches along the hydrological network of Artikutza: four control (C1, C2, C3, and C4) monitoring reaches, one upstream from the dam and three in free-flowing tributaries, and four Impact (I1, I2, I3, and I4) reaches consecutively located downstream from the dam (Fig. 1). We studied all reaches Before the bottom gate of Enobieta Dam was opened (B, December 2018), during the drawdown process (D, December 2018 to December 2019) and after the reservoir was totally emptied (A, December 2019 to October 2020). All reaches were sampled at least two times within each period, although the weather and the Covid-19 pandemic mobility limitations prevented us from always sampling during the same seasons (Fig. 2).

Water Physicochemical Characteristics

We measured turbidity in nephelometric turbidity units (NTUs) every 10 minutes from July 2018 to September 2020 by means of two turbidimeters (Solitax sc Sensor, Hach Company, U.S.A.) installed 30 m apart: one at reach I2 and the other at reach C2, which have a drainage area of 11.35 and 7.32 km^2, respectively.

On each sampling date and site, we measured water temperature (°C), dissolved oxygen (DO) saturation (%), electrical conductivity (EC, µS/cm), and pH with a handheld probe (Multi 3630 IDS, WTW, Germany). Additionally, we collected water samples. Samples for the determination of metal concentrations (iron [Fe, mg/L] and manganese [Mn, mg/L]) were fixed with 65% nitric acid (HNO_3) and stored in the fridge at 4°C until they were analyzed by inductively coupled plasma mass spectrometry (Fernández-Turiel et al. 2000). The rest of the samples were filtered through 0.7-µm-pore size precombusted fiberglass filters (Whatman GF/F, Whatman International, UK) and stored in the laboratory at −20°C until analysis. We determined soluble reactive phosphorus (SRP, µg P/L; molybdate method; Murphy & Riley 1962) and ammonium (NH_4^+ µg P/L; salicylate method; Reardon et al. 1966) by spectrophotometry (Shimadzu UV-1800 UV–Vis, Shimadzu Corporation, Japan).

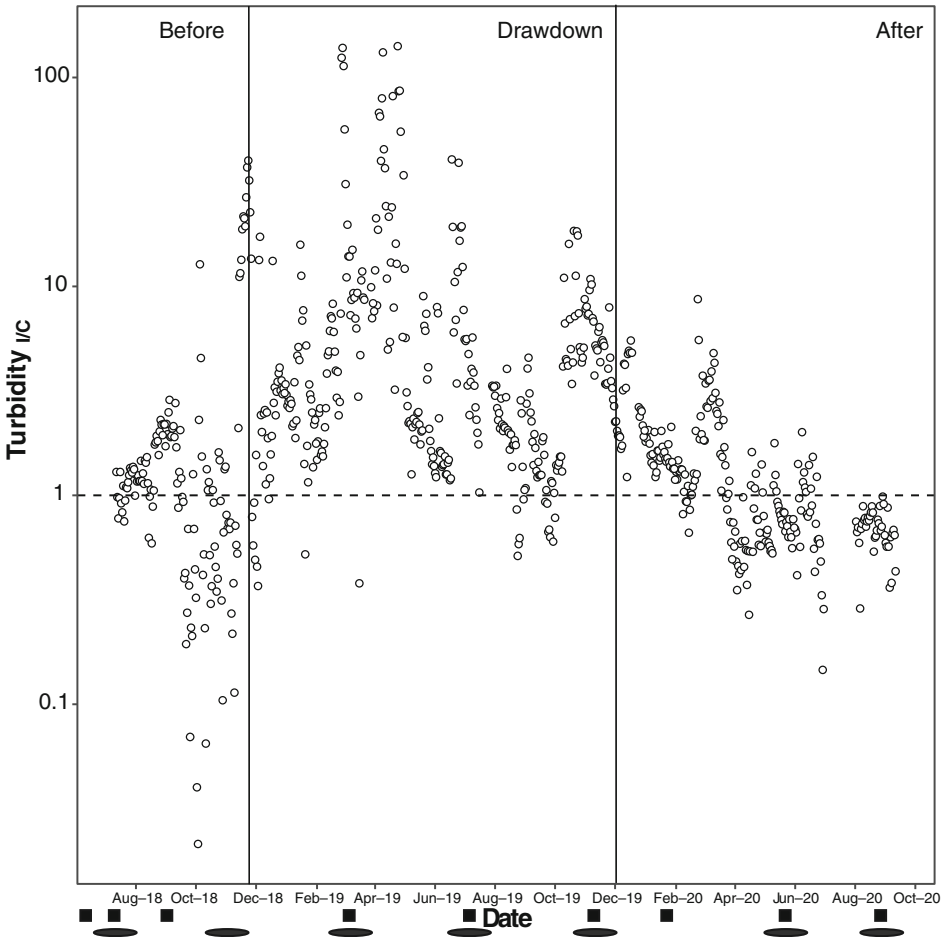

Figure 2. Turbidity time series data represented as impact/control (I/C) ratio during the before, drawdown, and after periods (separated by vertical lines). Values near the dashed line denote similar turbidity in impact and control reaches, with points above the line having higher turbidity in the impact reach. Black squares at the bottom indicate the dates of retrieval of biofilm carriers and ellipses the dates in which tongue depressors were retrieved. Note that the *y*-axis is in log scale.

Biofilm Structure and Functioning

We measured biofilm structure (i.e. biomass and Chl-*a*) and three benthic biofilm functions (i.e. metabolism, nutrient uptake, and organic matter decomposition) using standard substrata. For functions dominated by autotrophic biofilms (metabolism and nutrient uptake), we used biofilm carriers (51.45 cm^2, SERA GmbH D52518, Heinsberg, Germany) similar to those used in previous research (Elosegi et al. 2018; Pereda et al. 2020). For decomposition, dominated by heterotrophic biofilms, we used tongue depressors made of untreated poplar wood (*Populus nigra* × *canadiensis* Moench; 15 × 1.8 × 0.2 cm; Arroita et al. 2012). Approximately 2 months before the beginning of the experiment, we randomly deployed six biofilm carriers and five wooden sticks per reach tied with nylon line to metal bars or roots.

The biofilm carriers were used to determine biomass, Chl-*a*, metabolism, and nutrient uptake. We recovered them at least 2 months after deployment, and on each occasion, we deployed six more carriers to be colonized for the next sampling campaign. After collection, we stored the biofilm carriers in stream water inside plastic containers to carry them to the laboratory. These biofilm carriers were used in a bioassay to determine biofilm metabolism and nutrient uptake. Once in the laboratory, biofilm carriers were acclimatized to local conditions (10°C and 180 mmol m^{-2} $second^{-1}$ light) for 30 minutes in 500 mL of modified Chu culture medium (Andersen 2005). This medium is widely used for freshwater algal growth since it ensures the supply of essential macro- (e.g. nitrogen) and micronutrients (e.g. calcium, silica, or sodium) during the incubation. After acclimation, biofilm carriers were individually placed in light ($n = 3$ per site) and dark ($n = 3$ per site) 60-mL septa bottles completely filled with the same solution spiked with 10 mM solutions of phosphate (K_2HPO_4) and ammonium (NH_4Cl) to reach a final concentration of 5 µM (155 µg P/L and 70 µg N/L, respectively). These concentrations ensured saturating conditions for the biofilm and allowed estimating nutrient uptake from the concentration decline during the incubation. Then, we incubated the biofilm carriers for 2 hours under the same conditions of temperature and light as during acclimation. Noncolonized biofilm carriers were also incubated as blanks. Afterward, we measured DO concentrations with a portable fiber optic oxygen meter coupled to a syringe-like probe (Microsensor NTH-PSt7 on Microx4, Pre4Sens, Germany) and filtered (Whatman GF/F)

Table 1. Water characteristics in control reaches (C1, C2, C3, and C4) and impact reaches (I1, I2, I3, and I4) during periods before ($n = 7$), drawdown ($n = 6$), and after ($n = 3$). Values shown are mean ± standard error. Values in brackets represent the Ln-transformed ratio of the average for each impact site divided by the overall average of the control sites for each period.

		Reach							
Variable	*Period*	*C1*	*C2*	*C3*	*C4*	*I1*	*I2*	*I3*	*I4*
Fe (μg/L)	Before	18.1 ± 6	10 ± 0	15.5 ± 3.7	10 ± 0	131.4 ± 43.6 (2.28)	126.8 ± 63.3 (2.25)	54.9 ± 18.8 (1.41)	29.9 ± 7 (0.80)
	Drawdown	46.3 ± 14.4	10 ± 0	34 ± 16.7	62.3 ± 33.6	298.3 ± 127.7 (2.06)	233.2 ± 107.1 (1.81)	272.5 ± 137.3 (1.97)	36 ± 13.1 (−0.06)
	After	10 ± 0	42.3 ± 18.2	19.1 ± 4.7	17.4 ± 3.7	63.3 ± 15.9 (1.05)	32 ± 7.1 (0.37)	24 ± 6.4 (0.08)	15.5 ± 5.5 (−0.36)
Mn (μg/L)	Before	5 ± 0	5 ± 0	5 ± 0	5 ± 0	106.3 ± 30.5 (3.06)	85.8 ± 31 (2.84)	42.1 ± 19.3 (2.13)	15.9 ± 3.9 (1.16)
	Drawdown	8.3 ± 3.3	5 ± 0	21.7 ± 16.7	16.3 ± 7.2	131 ± 44 (2.32)	78.5 ± 27.9 (1.81)	105.1 ± 73.1 (2.10)	8.1 ± 3.1 (−0.46)
	After	5 ± 0	7.5 ± 2.5	5 ± 0	5 ± 0	31.6 ± 3.9 (1.73)	15.6 ± 0.9 (1.02)	5 ± 0 (−0.12)	5 ± 0 (−0.12)
EC (μS/cm)	Before	58.7 ± 1.9	60.9 ± 2.9	48.4 ± 1.9	105.2 ± 6.3	95.9 ± 9 (0.34)	83.3 ± 6.5 (0.20)	73.2 ± 5.5 (0.07)	85.8 ± 5.4 (0.24)
	Drawdown	61.3 ± 3.1	62.3 ± 1.9	50.2 ± 2	109.9 ± 8.1	103.4 ± 6.6 (0.39)	91.9 ± 6.5 (0.27)	76.7 ± 6 (0.09)	91.7 ± 7.2 (0.27)
	After	61.4 ± 2.5	66.8 ± 2.1	50.7 ± 1.1	110.4 ± 8.7	117.8 ± 8 (0.49)	98.5 ± 6.7 (0.31)	80.4 ± 5.5 (0.11)	94.1 ± 7.3 (0.26)
pH	Before	7.2 ± 0.2	7.4 ± 0.1	7.1 ± 0.2	7.5 ± 0.4	7.5 ± 0.1 (0.02)	7.5 ± 0.2 (0.02)	7.5 ± 0.1 (0.02)	7.7 ± 0.1 (0.05)
	Drawdown	7.2 ± 0.1	7.2 ± 0.1	7.2 ± 0.1	7.6 ± 0.1	7.4 ± 0.1 (0.01)	7.3 ± 0.1 (0)	7.4 ± 0.1 (0)	7.4 ± 0.2 (0.01)
	After	7.5 ± 0.3	7.6 ± 0.2	7.4 ± 0.3	7.6 ± 0.1	7.7 ± 0 (0.03)	7.6 ± 0.1 (0)	7.5 ± 0.1 (0)	7.3 ± 0.1 (−0.03)
DO sat. (%)	Before	99.7 ± 0.5	101.6 ± 0.5	101.1 ± 0.6	102.5 ± 0.5	100.1 ± 0.4 (−0.01)	101.6 ± 0.7 (0)	101.8 ± 0.5 (0)	102.5 ± 0.6 (0.01)
	Drawdown	100.1 ± 1.2	101.6 ± 0.6	100.4 ± 0.7	101.8 ± 0.6	100.1 ± 1.3 (0)	100.8 ± 0.7 (0)	101.2 ± 0.7 (0)	101.5 ± 1.1 (0)
	After	102 ± 1.2	101.1 ± 0.4	100.7 ± 0.2	101.7 ± 0.1	101.6 ± 0.1 (0)	101.9 ± 0.2 (0)	100.9 ± 0.5 (0)	101.1 ± 0.1 (0)
T (°C)	Before	11.3 ± 1	11.2 ± 1.2	11.4 ± 1.1	11.5 ± 0.8	13.3 ± 1.6 (0.16)	12.5 ± 1.4 (0.10)	12.4 ± 1.3 (0.09)	12.2 ± 1.1 (0.07)
	Drawdown	12.2 ± 1.3	12.5 ± 1.4	11.8 ± 1.5	11.9 ± 1	13.8 ± 1.8 (0.13)	12.6 ± 1.1 (0.04)	12.5 ± 1.4 (0.03)	12.2 ± 1.3 (0.01)
	After	11.7 ± 2.1	10.9 ± 2.5	10.2 ± 2.1	10.2 ± 1.3	12.9 ± 2.6 (0.18)	11.7 ± 2.2 (0.08)	10.5 ± 2 (−0.02)	9.7 ± 1.3 (−0.10)
SRP (μg/L)	Before	17.3 ± 5.1	8.8 ± 35.8	16.4 ± 8.6	12.9 ± 8.3	14.8 ± 12.4 (−0.06)	11.3 ± 7.3 (−0.21)	11.6 ± 7.2 (−0.18)	12.9 ± 8.3 (−0.07)
	Drawdown	9.2 ± 2	12.5 ± 1.1	12.6 ± 1.9	9.2 ± 2.7	6.4 ± 1.3 (−0.30)	6.1 ± 1.8 (−0.36)	9.9 ± 2.4 (0.13)	10.3 ± 3 (0.17)
	After	8.3 ± 2.3	10.9 ± 3	8.35 ± 3.9	5.2 ± 0.7	6 ± 1.5 (0.18)	4.4 ± 1.5 (0.08)	5.2 ± 0.7 (−0.02)	6 ± 1.5 (−0.10)
NH_4^+ (μg/L)	Before	3.3 ± 0.8	4.9 ± 1.6	7.8 ± 3.1	5.4 ± 2.1	21.1 ± 7.5 (1.37)	16.3 ± 5.5 (1.12)	8.4 ± 2.8 (0.45)	7.5 ± 1.8 (0.33)
	Drawdown	15.6 ± 5.7	21 ± 7.3	7.9 ± 2.3	11.7 ± 3.3	61.4 ± 37.3 (1.45)	20 ± 6.1 (1.06)	9 ± 2 (0.26)	13.7 ± 6.6 (0.19)
	After	2.5 ± 0	2.5 ± 0	2.5 ± 0	2.5 ± 0	2.5 ± 0 (0)	2.5 ± 0 (0)	2.5 ± 0 (0)	2.5 ± 0 (0)

Table 2. Results of the linear mixed-effects models using period (before/drawdown/after) and reach (control/impact) as fixed factors and water physicochemical attributes as response variables. Sampling date within each period and sampling site were used as random factors. Bold values indicate statistically significant results with $p < 0.05$. Degrees of freedom were estimated with Satterthwaite's method.

Variable	*Source of Variation*	*df*	*F*	*p*
Fe (µg/L)	BDA	2, 10	2.3	0.15
	CI	1, 6.22	12.2	**<0.05**
	BDA:CI	2, 82	8.77	**<0.001**
Mn (µg/L)	BDA	2, 10	2.75	0.11
	CI	1, 6.16	10.68	**<0.05**
	BDA:CI	2, 82	9.01	**<0.001**
EC (µS/cm)	BDA	2, 12.06	0.7	0.52
	CI	1, 6.03	2.16	0.19
	BDA:CI	2, 89.2	2.83	0.06
pH	BDA	2, 11.94	0.35	0.71
	CI	1, 7.35	1.09	0.33
	BDA:CI	2, 90.03	1.77	0.18
O_2 sat. (%)	BDA	2, 11.95	0.17	0.85
	CI	1, 6.56	0.02	0.9
	BDA:CI	2, 91.03	0.25	0.78
T (°C)	BDA	2, 12.01	0.23	0.8
	CI	1, 6.66	5.28	0.06
	BDA:CI	2, 91.02	2.86	0.06
SRP (µg/L)	BDA	2, 9	0.1	0.91
	CI	1, 6.21	0.23	0.65
	BDA:CI	2, 74.03	2.5	0.09
NH_4^+ (µg/L)	BDA	2, 10.02	7.23	**<0.05**
	CI	1, 7.1	4.29	0.08
	BDA:CI	2, 81.13	2.44	0.09

20 mL of solution for SRP and NH_4^+ analyses for each bottle (colonized and noncolonized). Biofilm metabolism was calculated from the difference in DO concentration between colonized and noncolonized bottles and expressed based on the incubation time interval and accounting for the water volume in the bottle and the surface of the biofilm carrier (mg O_2 hour^{-1} m^{-2}). Changes in DO concentration in light bottles were used to compute net community production (NCP) and those in dark bottles to compute community respiration (CR). Gross primary production (GPP) was calculated as the sum of NCP and CR (Hall & Hotchkiss 2017). The uptake of SRP and NH_4^+ was calculated as the difference between the mean SRP and NH_4^+ concentration of the control (i.e. noncolonized) and the colonized substrates and accounting for the incubation volume and time and then expressed per surface unit (µg P hour^{-1} m^{-2} and µg N hour^{-1} m^{-2}) (Elosegi et al. 2018). Since we did not detect any differences between light and dark bottles, SRP and NH_4^+ uptake rates calculated from both light and dark bottles were used as replicates to determine average biofilm uptake per reach and date.

Once incubations were finalized, all biofilm carriers were frozen at −20°C until analysis of biomass and Chl-*a*. We scraped the biofilm carriers in 100 mL of deionized water and divided the obtained slurry into two subsamples for biomass and Chl-*a* determination (50 mL each, approximately), which were filtered through preweighed and precombusted filters (0.7-µm pore size). Filters for biomass determination were oven-dried (70°C, 72 hours), weighed, ashed (500°C, 5 hours) and weighed again to estimate ash-free dry mass (AFDM). This value was corrected by the fraction of the filtered subsample to total sample and divided by the area of the biofilm carriers to express the result per surface unit (g AFDM/m^2). For Chl-*a* extraction and quantification, filters were placed in 90% v/v acetone overnight at 4°C and the extracted samples were measured spectrophotometrically (Shimadzu UV-1800 UV–Vis) (Steinman et al. 2017) after sonicating (3 minutes; Selecta sonication bath, operating at 360 W power, 50/60 Hz

Table 3. Results of the linear mixed-effects models using period (before/drawdown/after) and reach (control/impact) as fixed factors and biofilm structural and functional attributes as response variables. Sampling date within each period and sampling site were used as random factors. Bold values indicate statistically significant results with $p < 0.05$. Degrees of freedom were estimated with Satterthwaite's method.

Variable	*Source of Variation*	*df*	*F*	*p*
Biomass (g AFDM/m^2)	BDA	2, 4.01	3.24	0.15
	CI	1, 6.72	0.6	0.47
	BDA:CI	2, 259.78	0.65	0.52
Chlorophyll-*a* (mg/m^2)	BDA	2, 4	0.34	0.73
	CI	1, 6.83	3.41	0.11
	BDA:CI	2, 271.6	6.14	**<0.01**
GPP (mg O_2 hour^{-1} m^{-2})	BDA	2, 6	1.4	0.32
	CI	1, 6	2.89	0.14
	BDA:CI	2, 54	14.15	**<0.0001**
CR (mg O_2 hour^{-1} m^{-2})	BDA	2, 6.02	0.87	0.47
	CI	1, 5.93	1.16	0.32
	BDA:CI	2, 163.6	16.12	**<0.0001**
SRP (µg hour^{-1} m^{-2})	BDA	2, 5	1.23	0.37
	CI	1, 6	4.35	0.08
	BDA:CI	2, 162.2	0.4	0.67
NH_4^+ uptake (µg hour^{-1} m^{-2})	BDA	2, 5.02	1.74	0.27
	CI	1, 6.04	0.04	0.86
	BDA:CI	2, 161.14	0.01	0.99
k (day^{-1})	BDA	2, 4.05	0.99	0.45
	CI	1, 6.37	5.39	0.06
	BDA:CI	2, 221.6	1.97	0.14

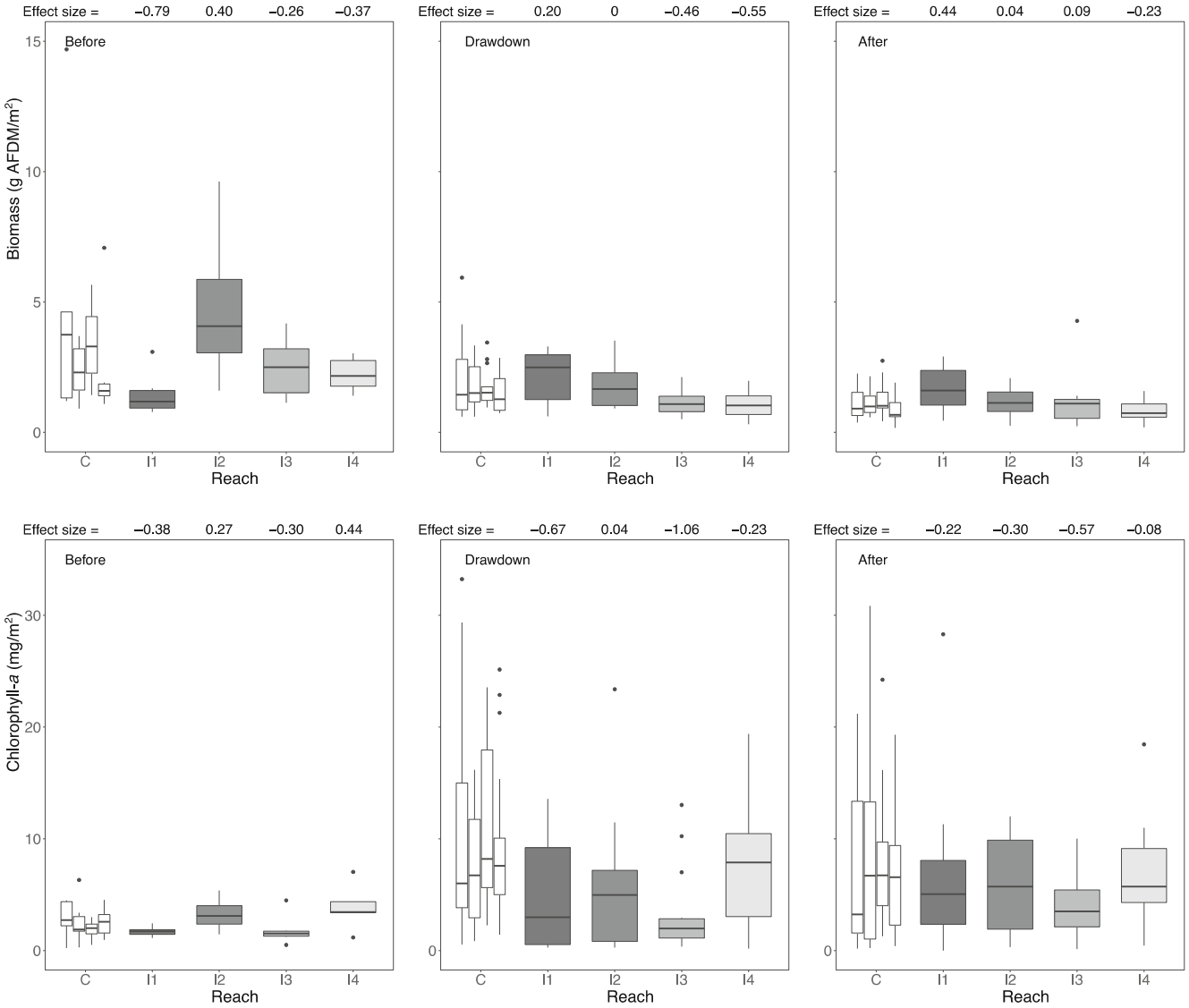

Figure 3. Biofilm biomass (top panels) and Chl-*a* concentration (lower panels) in control and impact reaches before, during, and after the drawdown. The box plots show the median, the interquartile range, and the tails of the distribution, and dots represent outliers. C represents results for each control reach (C1 to C4 from left to right). I1 to I4 represent results for each impact reach. The gray scale reflects distance from the dam. Effect sizes on top represent the Ln-transformed ratio of the average of each impact site divided by the overall average of the control sites for each period.

frequency, JP Selecta S.A., Spain) and centrifuging (2,000 rpm, 10 minutes; P-Selecta Mixtasel, JP Selecta S.A., Spain). We corrected Chl-*a* values by the fraction of the filtered subsample to total sample and divided by the area of the biofilm carriers to express the result per surface unit (mg Chl-*a*/m^2).

The wooden tongue depressors were used to determine organic matter decomposition. Before deployment, they were first punched to make a hole for later tying them with nylon line to metal bars and then oven-dried (70°C, 72 hours) and individually weighed. Every 4 months after deployment, they were recovered and replaced by new ones for the next sampling occasion. Upon recovery, depressors were rinsed with tap water to remove attached invertebrates and mineral particles before the AFDM was measured by gravimetry as done for biofilm AFDM (72 hours at 70°C, 5 hours at 500°C). To convert initial dry mass to AFDM, unexposed depressors were placed in tap water for 24 hours after which they were analyzed following the methods of deployed depressors. Organic matter decomposition rate (k, day^{-1}) was calculated assuming the negative exponential model (Petersen & Cummins 1974) using the calculated initial AFDM from the regression and the measured end AFDM and the length of deployment.

Data Analysis

To determine the effect of the dam removal on downstream reaches, we compared control and impact reaches for the three periods. Specifically, we used linear mixed-effects (lme) models

with restricted maximum likelihood (Pinheiro & Bates 2006) for all the variables except turbidity, using period (before/drawdown/after [BDA]) and reach (control/impact [CI]) as fixed factors. Sampling date within each period and sampling site were used as random factors in the models. All the models were fit using the "lmer" function of the "lme4" package in R (Bates et al. 2015). The overall effect of the drawdown was shown by the interaction between period and reach (BDA:CI). To further explore the effect of the reservoir drawdown and the afterward restoration success, we observed the full output of each lme model using the "summary" function in R. Considering that the intercept for the fixed factors was control reaches during the before period, from the full output we extracted (1) control-impact comparison during the before period (BCI) to determine whether there was any effect on the impact reaches previous to the reservoir drawdown, (2) the before-drawdown/control-impact (BD:CI) interaction to determine whether the drawdown of the reservoir had any effect on the impact reaches, and (3) the before-after/control-impact (BA:CI) interaction to determine whether impact reaches recovered from the effects of the reservoir drawdown. In all cases, we assessed the behavior of residuals to avoid departures from normality and homoscedasticity in the models. If data did not meet these specifications, variables were log transformed to fulfill the requirements of the parametric analyses. To minimize the use of binary significance language, instead of using the arbitrary $p = 0.05$ threshold, we describe statistical results using a gradual language of evidence (Muff et al. 2022).

Additionally, to test whether the effects of the dam and its decommissioning decreased downstream, we calculated effect

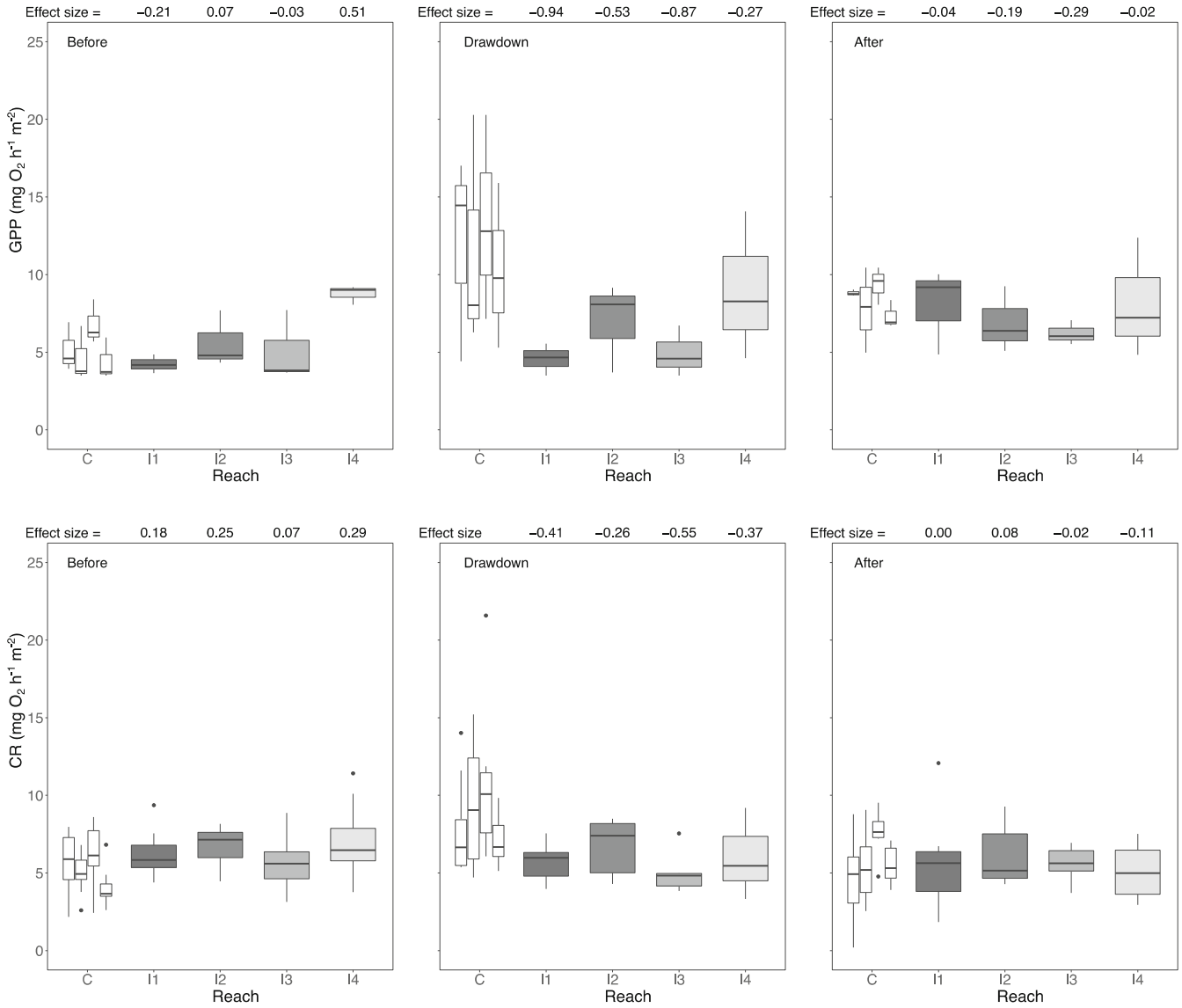

Figure 4. Biofilm gross primary production (GPP; top panels) and community respiration (CR; lower panels) in control and impact reaches before, during, and after the drawdown. The box plots show the median, the interquartile range, and the tails of the distribution, and dots represent outliers. C represents results for each control reach (C1 to C4 from left to right). I1 to I4 represent results for each impact reach. The gray scale reflects distance from the dam. Effect sizes on top represent the Ln-transformed ratio of the average for each impact site divided by the overall average of the control sites for each period.

sizes for all variables and periods as Ln-ratios between the value at each impact site and the average among all control values. Negative values of the ratio indicate reduced values below the dam, whereas positive values show increases. All statistical analyses and figures were done with R software (version 4.0.3; R Core Team 2020).

Results

Water Physicochemical Characteristics

During the before period, both control and impact reaches showed similar turbidity values (median: control before = 0.93 NTU, impact before = 1.01 NTU) resulting in I/C ratios near 1 (Fig. 2). When the bottom gate was first opened in December 2018, turbidity in the Impact reach increased remarkably (up to 292 NTU) due to sediment released from the reservoir. Frequent turbidity peaks occurred during the rest of the drawdown period (median: control drawdown = 0.82 NTU, impact drawdown = 2.86 NTU), when adjustments in the newly formed channel upstream from the dam triggered sediment transport. The last noticeable turbidity peak happened when the small weir within the reservoir was removed in October 2019. After this episode, no more turbidity peaks derived from the reservoir were noticed during the after period (median: control after: 1.39 NTU, impact after: 1.15 NTU).

There was strong evidence that the drawdown of the reservoir altered total Fe and Mn (BDA:CI_{Fe} $p < 0.001$; BDA:CI_{Mn}

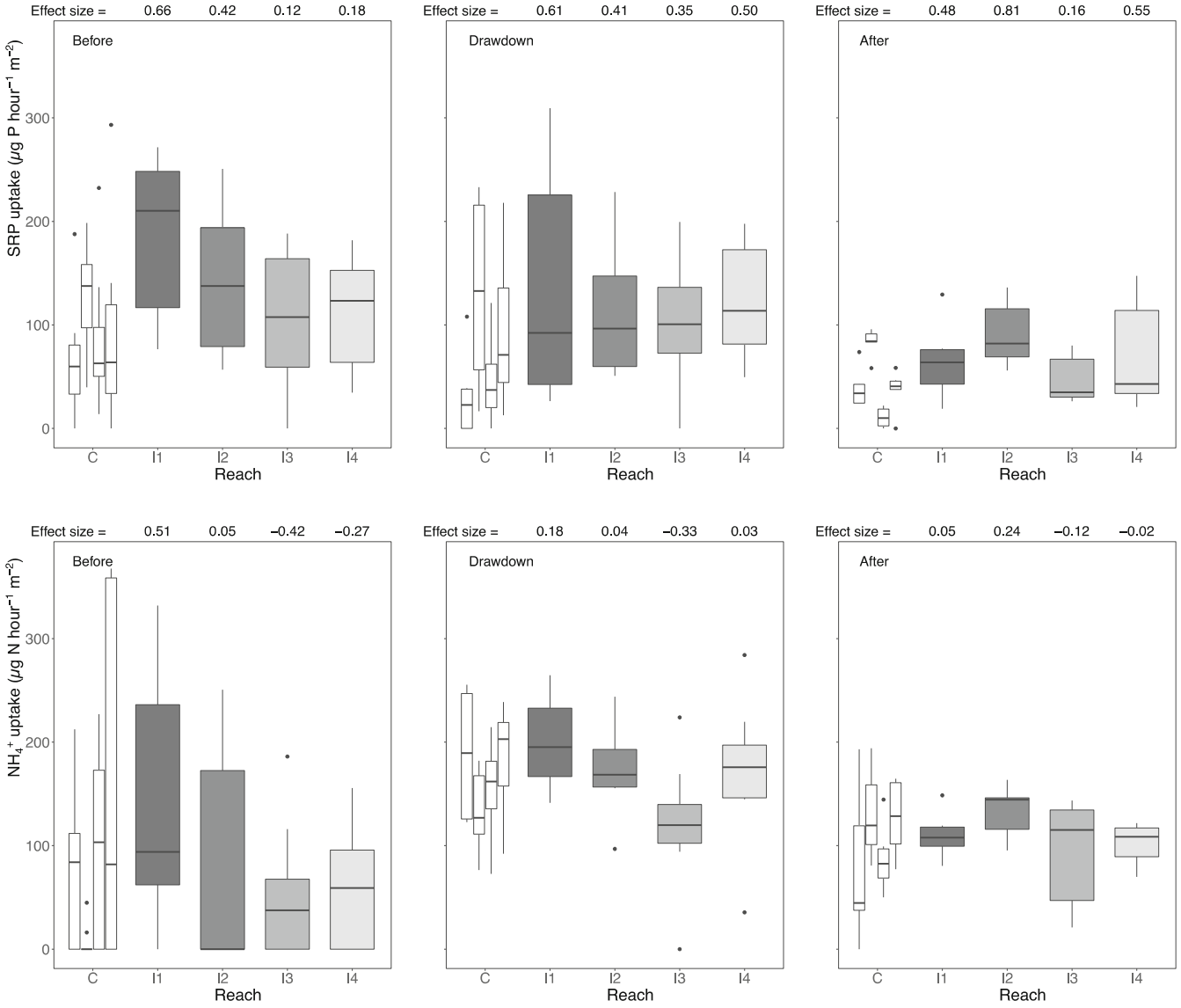

Figure 5. Biofilm uptake of soluble reactive phosphorus (SRP; top panels) and ammonium (NH_4^+; lower panels) in control and impact reaches before, during, and after the drawdown. The box plots show the median, the interquartile range, and the tails of the distribution, and dots represent outliers. C represents results for each control reach (C1 to C4 from left to right). I1 to I4 represent results for each impact reach. The gray scale reflects distance from the dam. Effect sizes on top represent the Ln-transformed ratio of the average for each impact site divided by the overall average of the control sites for each period.

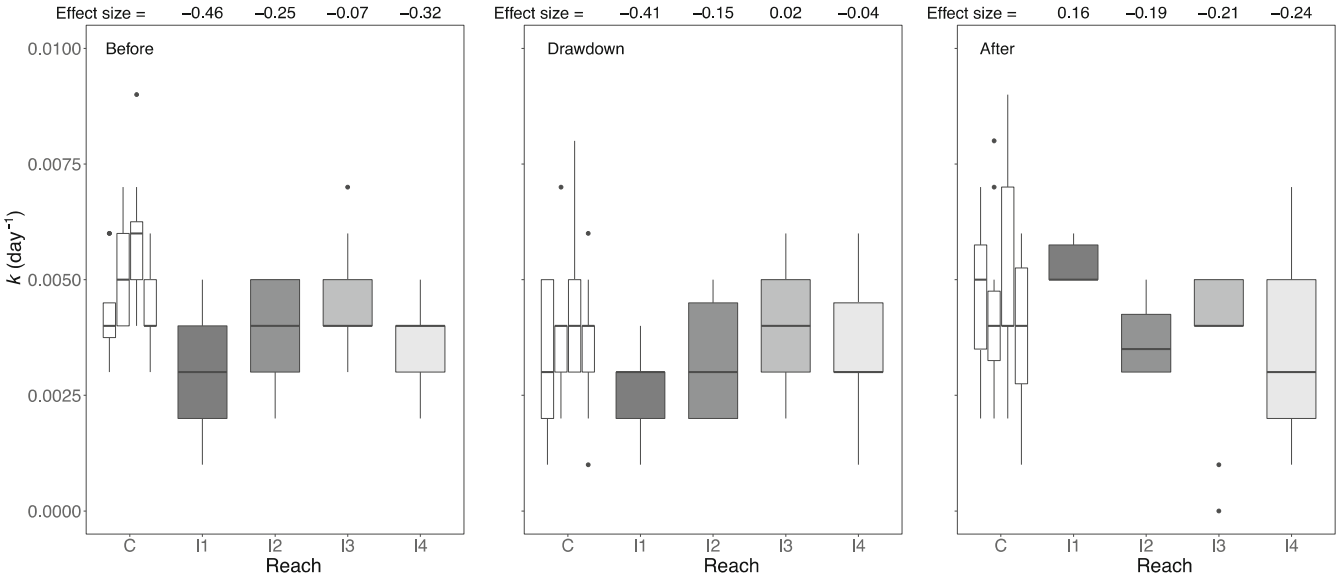

Figure 6. Organic matter decomposition rate (k) in control and impact reaches before, during, and after the drawdown. The box plots show the median, the interquartile range, and the tails of the distribution, and dots represent outliers. C represents results for each control reach (C1 to C4 from left to right). I1 to I4 represent results for each impact reach. The gray scale reflects distance from the dam. Effect sizes on top represent the Ln-transformed ratio of the average for each impact site divided by the overall average of the control sites for each period.

$p < 0.001$; Table 2). During the before period, Fe and Mn concentrations were higher in the impact reaches (BCI_{Fe} $p < 0.01$; BCI_{Mn} $p < 0.01$; Table S1), especially in I1 (effect $size_{Fe} = 2.28$; effect $size_{Mn} = 3.06$) and I2 (effect $size_{Fe} = 2.25$; effect $size_{Mn} = 2.84$) (Table 1). Differences between control and impact reaches were maintained during the drawdown period as shown by the nonsignificant before-drawdown/control-impact interaction ($BD:CI_{Fe}$ $p = 0.96$; $BD:CI_{Mn}$ $p = 0.31$; Table S1) although effect size values decreased (Table 1). During the after period, data revealed strong evidence that Fe and Mn concentrations were reduced to nearby undammed reach values ($BA:CI_{Fe}$ $p < 0.01$; $BA:CI_{Mn}$ $p < 0.0001$; Table S1), as shown also by effects size values near or below 1 (Table 1).

There was weak evidence that the drawdown of the reservoir altered nutrient concentrations (SRP and NH_4^+), EC or T (Table 2). NH_4^+ concentration followed the clearest pattern related to the drawdown of the reservoir (Table 1). During the before period, comparison between control and impact reaches showed evidence that concentrations were, on average, higher in the impact reaches (BCI_{NH4+} $p < 0.01$; Table S1). According to effect size values, such effect was highest in reach I1 (effect size = 1.37) and lowest in reach I4 (effect size = 0.33). This pattern was maintained during the drawdown period ($BD:CI_{NH4+}$ $p = 0.40$; Table S1), but data revealed evidence that during the after period NH_4^+ concentrations were reduced to the point that they were similar in control and impact reaches ($BA:CI_{NH4+}$ $p < 0.05$) (Tables S1 and 1). On the contrary, there was lack of evidence that during the before period SRP concentrations were different in control and impact reaches (BCI_{SRP} $p = 0.24$; Table S1), although effect size values suggested that concentrations were lower in the impact reaches (Table 1). Overall, during the drawdown and the after periods SRP concentrations decreased more in the control than in the impact reaches ($BD:CI_{SRP}$ $p = 0.06$; $BA:CI_{SRP}$ $p = 0.10$; Table S1), differences between reach types becoming very small (Table 1). Finally, the data did not yield any evidence that the drawdown of the reservoir affected pH or DO saturation (Table 2).

Biofilm Structure and Functioning

Comparison between control and impact sites showed no evidence that the drawdown of the reservoir affected biofilm biomass ($BDA:CI_{Biomass}$ $p = 0.52$; Table 3). Indeed, values were similar in control and impact reaches during the before (mean ± SE = 3.24 ± 0.68 g AFDM/m^2 and 2.58 ± 0.43 g AFDM/m^2, respectively), drawdown (1.77 ± 0.14 g AFDM/m^2 and 1.46 ± 0.11 g AFDM/m^2) and after periods (1.08 ± 0.07 g AFDM/m^2 and 1.21 ± 0.10 g AFDM/m^2; Fig. 3). Nevertheless, effect sizes indicated that in reach I1 biofilm biomass was lower than in the control reaches during the before period, whereas it was higher during and after the drawdown of the reservoir (Fig. 3).

Contrasting with biomass, we found evidence that the drawdown of the reservoir altered biofilm Chl-*a* concentration ($BDA:CI_{Chl\text{-}a}$ $p < 0.01$; Table 3). During the before period, Chl-*a* showed similar values in the control and impact reaches (mean ± SE = 2.49 ± 0.34 mg/m^2 and 2.58 ± 0.43 mg/m^2, respectively) ($BCI_{Chl\text{-}a}$ $p = 0.86$; Table S2), but the drawdown of the reservoir reduced Chl-*a* by 44% in impact relative to control reaches (9.86 ± 0.99 and 5.56 ± 0.74 mg/m^2) ($BD:CI_{Chl\text{-}a}$ $p < 0.01$; Table S2; Fig. 3). This negative effect decreased during the after period, when Chl-*a* concentration showed again similar values in control and impact reaches (7.48 ± 0.84 mg/m^2 and 5.81 ± 0.63 mg/m^2) ($BA:CI_{Chl\text{-}a}$ $p = 0.27$; Table S2).

Effect sizes also showed this trend in biofilm Chl-*a* concentration, and I1 and I3 were the reaches most negatively affected during all three periods.

There was very strong evidence for a negative effect of the reservoir drawdown on biofilm metabolism (BDA:CI_{GPP} $p < 0.0001$; BDA:CI_{CR} $p < 0.0001$; Table 3; Fig. 4). GPP and CR were, respectively, 48 and 32% lower in the impact reaches during the drawdown period (BD:CI_{GPP} $p < 0.001$; BD:CI_{CR} $p < 0.001$; Table S2), and showed a recovery trend during the after period (BA:CI_{GPP} $p = 0.06$; BA:CI_{CR} $p = 0.07$; Table S2; Fig. 4). Effect sizes indicated that the negative effect of the drawdown of the reservoir was highest just below the dam and decreased downstream (Fig. 4).

Reservoir drawdown had minor effects on biofilm nutrient uptake (BDA:$CI_{SRPUptake}$ $p = 0.67$; BDA:CI_{NH4+} $p = 0.99$; Table 3; Fig. 5). During the Before period data revealed weak evidence that SRP uptake was higher in the impact reaches (mean ± SE = 133.76 ± 12.49 µg P $hour^{-1}$ m^{-2}) than in the control reaches (92.79 ± 11.37 µg P $hour^{-1}$ m^{-2}) ($BCI_{SRPUptake}$ $p = 0.07$; Table S2), but not NH_4^+ uptake (80.89 ± 18.68 µg P $hour^{-1}$ m^{-2} and 83.68 ± 15.50 µg P $hour^{-1}$ m^{-2}) ($BCI_{NH4+Uptake}$ $p = 0.82$; Table S2). Although data did not reveal any evidence that NH_4^+ uptake changed due to the drawdown (Table 3), effect sizes indicated that differences between control and impact reaches decreased from the before to the drawdown and the after periods (Fig. 5). By contrast, this ratio was quite constant within the whole study in the case of biofilm SRP uptake (Fig. 5).

Overall, there was no clear evidence that reservoir drawdown affected organic matter decomposition (BDA:CI_k $p = 0.15$; Table 3). However, the specific interactions differed depending on the period (BD:CI_k $p = 0.05$; BA:CI_k $p = 0.22$; Table S2). During the before period, comparison between control and impact reaches showed evidence that decomposition rates were lower below the dam (BCI $p < 0.01$; Table S2), and I1 was the most impaired reach (effect size = −0.46; Fig. 6).

Discussion

Aging large dams and reservoirs represent a big challenge for water managers (Perera et al. 2021), but still little is known on the immediate, mid-, and long-term effects of their decommissioning on stream biodiversity and ecosystem functioning. Following a mBACI design, our study allowed us to provide novel insights on the short-term impacts of reservoir drawdown, the first step toward dam decommissioning, on biofilm, a key component of stream ecosystems. Overall, our results showed that prior to decommissioning, the Enobieta Dam had negative effects on water quality, although these effects were greatly attenuated downstream along our study section. These changes in water quality seemed to affect biofilm structure and functioning. Drawdown caused subtle additional impacts, but these were small, likely because the slow drawdown prevented major turbidity events, and biofilm recovered fast afterward.

The main concerns regarding the drawdown of the Enobieta Reservoir were the potential impacts that the sediment released might cause downstream. First, the potential impact on biodiversity, as suspended solids can have detrimental effects on riverine communities (Wood & Armitage 1997; Izagirre et al. 2009; Davis et al. 2018), to the point that they are included among the most prevalent contaminants in streams (USEPA 2000). Second, the adverse effects that the sediment released might cause in the Añarbe Reservoir, located circa 15 km further downstream. Nevertheless, these concerns were minor since the stored sediment were not polluted (Ekos 2016) and their total volume did not exceed 88,000 m^3 (Girder 2016), which amounts to only 71.5% of the annual inputs to Añarbe Reservoir, estimated at 123,000 m^3 per year (CEDEX 2005). In any case, drawdown of the Enobieta Reservoir was slow and progressive to allow the stabilization of the emerging sediment by the colonizing vegetation before the bottom gate was opened, and thus, to minimize the volume of sediment exported. Indeed, by the time that the bottom gate was opened, the percentage (%) area of the impounded water was 10.6%, while exposed sediments and running water occupied, respectively, 86.8% 2.8% of the total area (Mabano et al. 2022). Thus, most exported sediments were mobilized as the Enobieta Stream carved a narrow channel through the exposed sediments, whereas the rest of the reservoir sediment stayed in place (Elosegi et al. 2022). It is remarkable that the channel so formed mainly followed the ancient channel, as shown by the remnants of buried riparian tree stumps. A similar strategy was followed in the Elwha River restoration project, where the Glines Canyon Dam and the Elwha Dam were removed following a top-down demolition strategy over 2–3 years to avoid turbidity peaks above 40,000 NTU, which would clog a downstream water treatment plant (Randle et al. 2015). The fact that turbidity below Enobieta did not exceed 700 NTU during drawdown points to the success of the strategy to reduce the movement of sediments. The temperate and moist climate, which promotes vegetation colonization, probably was also important to stabilize the sediments. The peak values of turbidity measured during drawdown of the Enobieta Reservoir were high for streams in Artikutza, where the extensive forest cover results in very low turbidity values (Larrañaga et al. 2019), but not uncommon during floods in other streams of the region (Zabaleta et al. 2007).

Suspended solids are not the only water quality variable affected by dams (Dević 2015) and their decommissioning (Ahearn & Dahlgren 2005; Foley et al. 2015). During their operational lifespan, seasonal stratification and hypolimnetic hypoxia cause many reservoirs to release high concentrations of metals such as Fe and Mn (Friedl & Wüest 2002; Munger et al. 2017). In Artikutza, total metal concentrations during the before period were high below the Enobieta Dam, especially in reach I1, where Fe and Mn levels were, on average, 10 and 21 times higher than in control reaches respectively (mean ± SE = 131.4 ± 43.6 µg Fe/L and 106.3 ± 30.5 µg Mn/L). Such values exceeded the European Drinking Water Directive standards (200 µg Fe/L and 50 µg Mn/L) (EU Directive 2020/2184). Drawdown of the Enobieta Reservoir increased Fe and Mn concentrations to values that even exceeded the 1,000 µg Fe/L threshold during some stages (e.g. when the bottom gate was first opened), but were limited

to short episodes. Water quality improved swiftly after drawdown, reaching by the end of the experiment the values of nearby undammed reaches for most variables.

Biofilms are highly sensitive to environmental changes (Battin et al. 2016), so such metal concentrations below the dam may have negatively affected biofilm structure and functioning, both during its operation and decommissioning. Indeed, against the pattern most often found below dams (Munn & Brusven 2004; Ponsatí et al. 2015), neither biofilm biomass or Chl-*a* nor metabolism were higher below Enobieta Dam, since Fe and Mn precipitating at circumneutral pH could have caused indirect physical impacts on benthic communities (Cadmus et al. 2018), such as sunlight blocking (Chon & Hwang 2000), in addition to direct toxic effects (Morin et al. 2012; Harford et al. 2015; Kosarev et al. 2022). Additionally, as it was maintained unused and full for decades, Enobieta Reservoir had little or no regulating effect, and it may not have offered enough hydrological stability to reduce scouring and consequently enhance biofilm growth below the dam. During drawdown, Chl-*a* and metabolism were reduced downstream from the Enobieta Dam, most probably as a response to the presence of suspended solids, as reported elsewhere for small decommissioned dams (Orr et al. 2008; Chang et al. 2017). Turbidity and deposition of fine sediment can affect biofilm communities in contrasting ways. On the one hand, they reduce light penetration into the benthos (Davies-Colley et al. 1992) as well as the availability of stable attachment surfaces (Wood & Armitage 1997), thus limiting periphyton accrual and metabolism (Davies-Colley et al. 1992; Aspray et al. 2017; Louhi et al. 2017). On the other hand, sediments can also act as fertilizers and promote biofilm biomass and metabolism (Baattrup-Pedersen et al. 2020). In fact, Pérez-Calpe et al. (2021), in an experiment in which they exposed indoor channels to fine sediments from the Enobieta Reservoir, showed these sediments to promote biofilm biomass and metabolic activity, suggesting a fertilizing effect of the nutrient leachates. The exact balance between the potential subsidy and stress effects of fine sediments thus seems to be dependent of site-specific conditions, such as water velocity and light availability. In our case, both high turbidity and scouring episodes, as well as flow disturbances derived from the drawdown of the reservoir reduced autotrophic biofilm biomass in the impact reaches. Anyway, such impacts disappeared during the recovery period because biofilms in sheltered microhabitats may have acted as sources for recolonization, thus confirming the high resilience of biofilm (Dzubakova et al. 2018). Contrary to Chl-*a*, biofilm biomass tended to increase during drawdown in I1. This could reflect that autotrophs were more affected by drawdown than heterotrophs, or that autotrophs had less Chl-*a* per biomass. Alternatively, it could be the result of biofilm carriers trapping organic sediment, thus increasing their AFDM, although visual inspection did not reinforce this possibility.

As expected, biofilm GPP was also reduced due to the loss of primary producers (i.e. lower Chl-*a*) during the drawdown of the reservoir. On the contrary, according to the increase in the AFDM, we could expect heterotrophs to be more resistant than autotrophs to the disturbances derived from the reservoir drawdown, and so, CR to be promoted, or at least, less affected than GPP. Based on our results, we are far from saying whether autotrophs were more affected than heterotrophs, but we hypothesize that in our case, CR was reduced, probably, due to the reduced autotrophic respiration as reported elsewhere (Uehlinger et al. 2003). Although metabolism was affected, drawdown exerted only subtle effects on nutrient uptake by the biofilm. During the before period, SRP uptake marginally higher in the reach closest to the dam and then decreased downstream. This longitudinal trend in SRP uptake was attenuated during the drawdown and after periods. In contrast, NH_4^+ uptake show no clear patterns. A potential explanation for these patterns is that the Enobieta Reservoir acted as a sink for phosphorus during its lifespan, as is reported for other impoundments (Ponsatí et al. 2015), as a consequence of sediment sequestering phosphorus (Maavara et al. 2015). This could result in phosphorus-starved biofilms below the dam during the before period, which, under our experimental conditions, resulted in high uptake (Reddy et al. 1999). The presence of more P-rich sediment in the reaches located below the dam during the after period might have decreased this P uptake potential. On the other hand, the fact that nitrogen was likely never the limiting nutrient in the study reaches might explain the lack of significant changes in biofilm NH_4^+ uptake among reaches and periods.

Similar to biofilm SRP uptake, during the before period heterotrophic microbial activity linked to organic matter breakdown was marginally different between control and impact reaches. Indeed, as in the case of biofilm metabolism, metal toxicity may have impaired decomposition below the dam. For instance, Lecerf and Chauvet (2008) showed metal pollution to reduce microbial decomposition of leaf litter and to depress spore production of aquatic fungi. Although we did not observe any clear pattern within the impact sites during and after reservoir drawdown, data revealed a slight increase of decomposition rates below the dam to the end of the experiment. This trend toward ecosystem functioning recovery may indicate that there was still a legacy effect of the previous degraded water quality state during the after period, and thus, that restoration to nearby undammed reaches conditions may take longer for microbial organic matter decomposition.

In summary, our results show that the slow drawdown of a large reservoir, a key step toward its final decommissioning, did not result in additional impacts to those caused by the operating reservoir. Furthermore, our findings indicate that biofilm biomass and activity recovered quickly afterward, reaching values similar to those in control reaches that are among the best-preserved streams in the region (Elosegi et al. 2019). Given the key role biofilms play on stream ecosystem functioning (Sabater et al. 2007; Battin et al. 2016) and the fact that the latter is the basis of essential ecosystem services, our results point to the beneficial effects of reservoir decommissioning on water quality and ecosystem services altogether, if carefully conducted to minimize impacts. This should be balanced with the efforts to restore the natural flux of other sediments such as gravel and cobbles, whose lack impairs ecosystems by "sediment starving" river sections below dams (Kondolf 1997;

Kondolf et al. 2014). In general, managers should strive to minimize the export of fine sediment stored beyond the ancient channel of the stream, by using a means to immobilize the sediments, as achieved through vegetation in this particular case.

Acknowledgments

This research was supported by the Fundación BBVA (064-17). The authors also acknowledge the financial support from the Basque Government (Consolidated Research Group: Stream Ecology 7-CA-18/10) predoctoral fellowships from the University of the Basque Country UPV/EHU (M.A.). The authors are especially grateful to the municipality of Donostia-San Sebastian and the staff of Artikutza for their continuous support during the experiment.

LITERATURE CITED

Ahearn DS, Dahlgren RA (2005) Sediment and nutrient dynamics following a low-head dam removal at Murphy Creek, California. Limnology and Oceanography 50:1752–1762. https://doi.org/10.4319/lo.2005.50.6.1752

Andersen RA (2005) Algal culturing techniques. Elsevier Academic Press, Cambridge, Massachusetts

Aristi I, Arroita M, Larrañaga A, Ponsatí L, Sabater S, von Schiller D, Elosegi A, Acuña V (2014) Flow regulation by dams affects ecosystem metabolism in Mediterranean rivers. Freshwater Biology 59:1816–1829. https://doi.org/10.1111/fwb.12385

Arroita M, Aristi I, Flores L, Larrañaga A, Díez J, Mora J, Roamí AM, Elosegi A (2012) The use of wooden sticks to assess stream ecosystem functioning: comparison with leaf breakdown rates. Science of the Total Environment 440:115–122. https://doi.org/10.1016/j.scitotenv.2012.07.090

Aspray KL, Holden J, Ledger ME, Mainstone CP, Brown LE (2017) Organic sediment pulses impact rivers across multiple levels of ecological organization. Ecohydrology 10:e1855. https://doi.org/10.1002/eco.1855

Baattrup-Pedersen A, Graeber D, Kallestrup H, Guo K, Rasmusse JJ, Larsen SE, Riis T (2020) Effects of low flow and co-occurring stressors on structural and functional characteristics of the benthic biofilm in small streams. Science of the Total Environment 733:139331. https://doi.org/10.1016/j.scitotenv.2020.139331

Bates D, Mächler M, Bolker B, Walker S (2015) Fitting linear mixed-effects models using lme4. Journal of Statistical Software 67:1–48. https://doi.org/10.18637/jss.v067.i01

Battin TJ, Besemer K, Bengtsson MM, Roamní AM, Packmann AI (2016) The ecology and biogeochemistry of stream biofilms. Nature Reviews Microbiology 14:251–263. https://doi.org/10.1038/nrmicro.2016.15

Bellmore JR, Duda JJ, Craig LS, Greene SL, Torgersen CE, Collins MJ, Vittum K (2017) Status and trends of dam removal research in the United States. Wiley Interdisciplinary Reviews: Water 4:e1164. https://doi.org/10.1002/wat2.1164

Bellmore JR, Pess GR, Duda JJ, O'Connor JE, East AW, Foley M, et al. (2019) Conceptualizing ecological responses to dam removal: if you remove it, what's to come? BioScience 69:12–14. https://doi.org/10.1093/biosci/biy152

Besemer K (2015) Biodiversity, community structure and function of biofilms in stream ecosystems. Research in Microbiology 166:774–781. https://doi.org/10.1016/j.resmic.2015.05.006

Cadmus P, Guasch H, Herdrich AT, Bonet B, Urrea G, Clements WH (2018) Structural and functional responses of periphyton and macroinvertebrate communities to ferric Fe, cu, and Zn in stream mesocosms. Environmental Toxicology and Chemistry 37:1320–1329. https://doi.org/10.1002/etc.4070

CEDEX (2005) Asistencia técnica para el estudio de la capacidad del embalse de Añarbe (Navarra). Technical report. CEDEX, Studies and Experimentation Centre, Spanish Government, Madrid.

Chang H-Y, Chiu M-C, Chuang Y-L, Tzeng C-S, Kuo M-H, Yeh C-H, et al. (2017) Community responses to dam removal in a subtropical mountainous stream. Aquatic Sciences 79:967–983. https://doi.org/10.1007/s00027-017-0545-0

Chon HT, Hwang JH (2000) Geochemical characteristics of the acid mine drainage in the water system in the vicinity of the Dogye coal mine in Korea. Environmental Geochemistry and Health 22:155–172. https://doi.org/10.1023/A:1006735226263

Colas F, Baudoin JM, Chauvet E, Clivot H, Danger M, Guérold F, Devin S (2016) Dam-associated multiple-stressor impacts on fungal biomass and richness reveal the initial signs of ecosystem functioning impairment. Ecological Indicators 60:1077–1090. https://doi.org/10.1016/j.ecolind.2015.08.027

Davies-Colley RJ, Hickey CW, Quinn JM, Ryan PA (1992) Effects of clay discharges on streams—1. Optical properties and epilithon. Hydrobiologia 248:215–234. https://doi.org/10.1007/BF00006149

Davis SJ, HUallacháin DÓ, Mellander P-E, Kelly A-M, Mathhaei CD, Piggot JJ, Kelly-Quinn M (2018) Multiple-stressor effects of sediment, phosphorus and nitrogen on stream macroinvertebrate communities. Science of the Total Environment 637–638:577–587. https://doi.org/10.1016/j.scitotenv.2018.05.052

Dević G (2015) Environmental impacts of reservoirs. Pages 561–575. In: Environmental indicators. Springer, Dordrecht, The Netherlands. https://doi.org/10.1007/978-94-017-9499-2_33

Dzubakova K, Peter H, Bertuzzo E, Juez C, Franca MJ, Rinaldo BTJ (2018) Environmental heterogeneity promotes spatial resilience of phototrophic biofilms in streambeds. Biology Letters 14:20180432. https://doi.org/10.1098/rsbl.2018.0432

Ekos (2016) Caracterización de los sedimentos del embalse de Artikutza y pautas para su gestión. Technical report for the Municipality of San Sebastian. Ekos, Donostia-San Sebastian.

Ellis LE, Jones NE (2013) Longitudinal trends in regulated rivers: a review and synthesis within the context of the serial discontinuity concept. Environmental Reviews 21:136–148. https://doi.org/10.1139/er-2012-0064

Elosegi A, Nicolás A, Richardson JS (2018) Priming of leaf litter decomposition by algae seems of minor importance in natural streams during autumn. PLoS One 13:e0200180. https://doi.org/10.1371/journal.pone.0200180

Elosegi A, Atristain M, Larrañaga A, von Schiller D (2019) Artikutzako errekak. Pages 316–333. In: Artikutza, natura eta historia. Donostiako udaleko Osasun eta Ingurumen Saila. Donostia - San Sebastian.

Elosegi A, González-Esteban J, Monfort R (2022) Evaluación de las distintas alternativas de puesta fuera de servicio de la presa de Enobieta sobre el estado de conservación de la ZEC ES2200010 Artikutza. Report for the Municipality of Donostia-San Sebastian

EU Directive 2020/2184 of the European Parliament and of the Council of 16 December 2020 on the quality of water intended for human consumption. DOUE-L-2020-81947.

Fernández-Turiel JL, Llorens JF, López-Vera F, Gómez-Artola C, Morell I, Gimeno D (2000) Strategy for water analysis using ICP-MS. Fresenius'-Journal of Analytical Chemistry 368:601–606. https://doi.org/10.1007/s002160000552

Foley MM, Duda JJ, Beirne MM, Paradis R, Ritchie A, Warrick JA (2015) Rapid water quality change in the Elwha River estuary complex during dam removal. Limnology and Oceanography 60:1719–1732. https://doi.org/10.1002/lno.10129

Foley MM, Bellmore JR, O'Connor JE, Duda JJ, East AE, Grant GE, et al. (2017) Dam removal: listening in. Water Resources Research 53:5229–5246. https://doi.org/10.1002/2017WR020457

Francoeur SN, Biggs BJF (2006) Short-term effects of elevated velocity and sediment abrasion on benthic algal communities. Hydrobiologia 561:59–69. https://doi.org/10.1007/s10750-005-1604-4

Friedl G, Wüest A (2002) Disrupting biogeochemical cycles—consequences of damming. Aquatic Sciences 64:55–65. https://doi.org/10.1007/s00027-002-8054-0

Girder (2016) Estudio de viabilidad de la puesta fuera de servicio de la presa de Artikutza. Technical report for the Municipality of San Sebastian. Girder Ingenieros. Donostia - San Sebastian.

Graf WL (2006) Downstream hydrologic and geomorphic effects of large dams on American rivers. Geomorphology 79:336–360. https://doi.org/10.1016/j.geomorph.2006.06.022

Habel M, Mechkin K, Podgorska K, Saunes M, Babiński Z, Chalov S, Absalon D, Podgórski Z, Obolewski K (2020) Dam and reservoir removal projects: a mix of social-ecological trends and cost-cutting attitudes. Scientific Reports 10:19210. https://doi.org/10.1038/s41598-020-76158-3

Hall RO, Hotchkiss ER (2017) Stream metabolism. Pages 219–233. In: Methods in stream ecology. Third edition. Vol 2. Academic Press.

Harford AJ, Mooney TJ, Trenfield MA, van Dam RA (2015) Manganese toxicity to tropical freshwater species in low hardness water. Environmental Toxicology and Chemistry 34:2856–2863. https://doi.org/10.1002/etc.3135

Hester ET, Doyle MW (2011) Human impacts to river temperature and their effects on biological processes: a quantitative synthesis. Journal of the American Water Resources Association 47:571–587. https://doi.org/10.1111/j.1752-1688.2011.00525.x

Izagirre O, Serra A, Guasch H, Elosegi A (2009) Effects of sediment deposition on periphytic biomass, photosynthetic activity and algal community structure. Science of the Total Environment 407:5694–5700. https://doi.org/10.1016/j.scitotenv.2009.06.049

Kondolf GM (1997) Hungry water: effects of dams and gravel mining on river channels. Environmental Management 21:533–551. https://doi.org/10.1007/s002679900048

Kondolf GM, Rubin ZK, Minear JT (2014) Dams on the Mekong: cumulative sediment starvation. Water Resources Research 50:5158–5169. https://doi.org/10.1002/2013WR014651

Kosarev AV, Ivanov DE, Kamenets AF (2022) The effect of manganese ions (II) on representatives of aquatic biota. IOP Conference Series: Earth and Environmental Science 949:012013. https://doi.org/10.1088/1755-1315/949/1/012013

Larrañaga A, Atristain M, von Schiller D, Elosegi A (2019) Artikutza (Navarra): diagnóstico ambiental de la red fluvial previo al desmantelamiento de un embalse y resultados preliminares del efecto del vaciado. Revista Digital del Cedex 193:4–15.

Lecerf A, Chauvet E (2008) Diversity and functions of leaf-decaying fungi in human-altered streams. Freshwater Biology 53:1658–1672. https://doi.org/10.1111/j.1365-2427.2008.01986.x

Louhi P, Richardson JS, Muotka T (2017) Sediment addition reduces the importance of predation on ecosystem functions in experimental stream channels. Canadian Journal of Fisheries and Aquatic Sciences 74:32–40. https://doi.org/10.1139/cjfas-2015-0530

Lozano P, Latasa I (2019) Vegetación. Pages 334–359. In: Artikutza, natura eta historia. Donostiako udaleko Osasun eta Ingurumen Saila. Donostia - San Sebastian.

Maavara T, Parsons CT, Ridenour C, Stojanovic S, Dür HH, Powley HR, van Cappellen P (2015) Global phosphorus retention by river damming. Proceedings of the National Academy of Sciences of the United States of America 112:15603–15608. https://doi.org/10.1073/pnas.1511797112

Maavara T, Chen Q, Van Meter K, Brown LE, Zhang J, Ni J, Zarfl C (2020) River dam impacts on biogeochemical cycling. Nature Reviews Earth and Environment 1:103–116. https://doi.org/10.1038/s43017-019-0019-0

Mabano A, von Schiller D, Suárez I, Atristain M, Elosegi A, Marcé R, García-Baquero G, Obrador B (2022) The drawdown phase of dam decommissioning is a hot moment of gaseous carbon emissions from a temperate reservoir. Inland waters 1–40. https://doi.org/10.1080/20442041.2022.2096977

Magilligan FJ, Grabe BE, Nislow KH, Chipman JW, Sneddon CS, Fox CA (2016) River restoration by dam removal: enhancing connectivity at watershed scales. Elementa 2016:108. https://doi.org/10.12952/journal.elementa.000108

Morin S, Cordonier A, Lavoie I, Arini A, Blanco S, Duong TT, et al. (2012) Consistency in diatom response to metal-contaminated environments. Pages 117–146. In: Handbook of environmental chemistry. Vol 19. Springer - Verlag, New York.

Morley SA, Coe JH DJJ, Kloehn KK, ML MH (2008) Benthic invertebrates and periphyton in the Elwha river basin: current conditions and predicted response to dam removal. Northwest Science 82:179–196. https://doi.org/10.3955/0029-344X-82.S.I.179

Muehlbauer JD, LeRoy CJ, JM LO, Flaccus KK, Vlieg JK, Marks JC (2009) Short-term responses of decomposers to flow restoration in Fossil Creek, Arizona, U.S.A. Hydrobiologia 618:35–45. https://doi.org/10.1007/s10750-008-9545-3

Muff S, Nilsen EB, O'hara RB, Nater CR (2022) Rewriting results sections in the language of evidence. Trends in Ecology & Evolution 37:203–210. https://doi.org/10.1016/j.tree.2021.10.009

Munger ZW, Shahady TD, Schreiber ME (2017) Effects of reservoir stratification and watershed hydrology on manganese and iron in a dam-regulated river. Hydrological Processes 31:1622–1635. https://doi.org/10.1002/hyp.11131

Munn MD, Brusven MA (2004) The influence of Dworshak Dam on epilithic community metabolism in the Clearwater River, U.S.A. Hydrobiologia 513:121–127. https://doi.org/10.1023/B:hydr.0000018177.78841.08

Murphy J, Riley JP (1962) A modified single solution method for the determination of phosphate in natural waters. Analytica Chimica Acta 27:31–36. https://doi.org/10.1016/S0003-2670(00)88444-5

Orr CH, Kroiss SJ, Rogers KL, Stanley EH (2008) Downstream benthic responses to small dam removal in a coldwater stream. River Research and Applications 24:804–822. https://doi.org/10.1002/rra.1084

Pereda O, Solagaistua L, Atristain M, de Guzmán I, Larrañaga A, von Schiller D, Elosegi A (2020) Impact of wastewater effluent pollution on stream functioning: a whole-ecosystem manipulation experiment. Environmental Pollution 258:113719. https://doi.org/10.1016/j.envpol.2019.113719

Perera D, Smakhtin V, Williams S, North T, Curry A (2021) Ageing water storage infrastructure: an emerging global risk. Report. United Nations University. Insitute for Water, Environment and Health (UNU-UNWEH). Hamilton.

Pérez-Calpe AV, Larrañaga A, von Schiller D, Elosegi A (2021) Interactive effects of discharge reduction and fine sediments on stream biofilm metabolism. PLoS One 16:e0246719. https://doi.org/10.1371/journal.pone.0246719

Petersen RC, Cummins KW (1974) Leaf processing in a woodland stream. Freshwater Biology 4:343–368. https://doi.org/10.1111/j.1365-2427.1974.tb00103.x

Pinheiro JC, Bates DM (2006) Linear mixed-effects models: basic concepts and examples. Pages 3–56. In: Mixed-effects models in S and S-PLUS. New York: Springer - Verlag.

Poff NLR, Allan JD, Bain MB, Karr JR, Prestegaard KL, Richter BD, Sparks RE, Stromberg JC (1997) The natural flow regime: a paradigm for river conservation and restoration. Bioscience 47:769–784. https://doi.org/10.2307/1313099

Ponsatí L, Acuña V, Aristi I, Arroita M, García-Berthou E, von Schiller D, Elosegi A, Sabater S (2015) Biofilm responses to flow regulation by dams in Mediterranean Rivers. River Research and Applications 31:1003–1016. https://doi.org/10.1002/rra.2807

R Core Team (2020) R: a language and environment for statistical computing. R Foundation for Statitistical Computing, Vienna, Austria. https://www.r-project.org/

Randle TJ, Bountry JA, Ritchie A, Wille K (2015) Large-scale dam removal on the Elwha River, Washington, U.S.A.: erosion of reservoir sediment. Geomorphology 246:709–728. https://doi.org/10.1016/j.geomorph.2014.12.045

Reardon J, Foreman JA, Searcy RL (1966) New reactants for the colorimetric determination of ammonia. Clinica Chimica Acta 14:403–405. https://doi.org/10.1016/0009-8981(66)90120-3

Reddy KR, Kadlec RH, Flaig E, Gale PM (1999) Phosphorus retention in streams and wetlands: a review. Critical Reviews in Environmental Science and Technology 29:83–146. https://doi.org/10.1080/10643389991259182

Sabater S, Guasch H, Ricart M, Romaní A, Vidal G, Klünder C, Schmitt-Jansen M (2007) Monitoring the effect of chemicals on biological communities: the biofilm as an interface. Analytical and Bioanalytical Chemistry 387:1425–1434. https://doi.org/10.1007/s00216-006-1051-8

von Schiller D, Aristi A, Ponsatí P, Arroita M, Acuña V, Elosegi A, Sabater S (2016) Regulation causes nitrogen cycling discontinuities in Mediterranean

rivers. Science of the Total Environment 540:168–177. https://doi.org/10.1016/j.scitotenv.2015.07.017

Smolar-Žvanut N, Mikoš M (2014) Impact de la régularisation du débit causée par les barrages hydroélectriques sur la communauté périphytique de la rivière Soca, Slovénie. Hydrological Sciences Journal 59:1032–1045. https://doi.org/10.1080/02626667.2013.834339

Steinman AD, McIntire CD (1990) Recovery of lotic periphyton communities after disturbance. Environmental Management 14:589–604. https://doi.org/10.1007/BF02394711

Steinman AD, Lamberti GA, Leavitt PR, Uzarski DG (2017) Biomass and pigments of benthic algae. Pages 223–241. In: Methods in stream ecology. Third edition. Vol 1. San Diego: Academic Press. https://doi.org/10.1016/B978-0-12-416558-8.00012-3

Tena A, Batalla RJ, Vericat D, López-Tarazón JA (2011) Suspended sediment dynamics in a large regulated river over a 10-year period (the lower Ebro, NE Iberian Peninsula). Geomorphology 125:73–84. https://doi.org/10.1016/j.geomorph.2010.07.029

Uehlinger U, Kawecka B, Robinson CT (2003) Effects of experimental floods on periphyton and stream metabolism below a high dam in the Swiss Alps (River Spöl). Aquatic Sciences 65:199–209. https://doi.org/10.1007/s00027-003-0664-7

Underwood AJ (1994) On beyond BACI: sampling designs that might reliably detect environmental disturbances. Ecological Applications 4:3–15. https://doi.org/10.2307/1942110

USEPA (2000) Nutrient criteria technical guidance manual: lakes and reservoirs. USEPA, Washington D.C.

Vericat D, Batalla RJ (2006) Sediment transport in a large impounded river: the lower Ebro, NE Iberian Peninsula. Geomorphology 79:72–92. https://doi.org/10.1016/j.geomorph.2005.09.017

Ward JV, Stanford JA (1983) Serial discontinuity concept of lotic ecosystems. Pages 29–42. In: Dynamics of lotic systems. Ann Arbor Science, Ann Arbor, Michigan

Wilcox AC, O'Connor JE, Major JJ (2014) Rapid reservoir erosion, hyperconcentrated flow, and downstream deposition triggered by breaching of 38 m tall Condit Dam, white Salmon River, Washington. Journal of Geophysical Research: Earth Surface 119:1376–1394. https://doi.org/10.1002/2013JF003073

Winton R, Calamita E, Wehrli B (2019) Reviews and syntheses: dams, water quality and tropical reservoir stratification. Biogeosciences 16:1657–1671. https://doi.org/10.5194/bg-16-1657-2019

Wood PJ, Armitage PD (1997) Biological effects of fine sediment in the lotic environment. Environmental Management 21:203–217. https://doi.org/10.1007/s002679900019

Wu H, Chen J, Xu J, Zeng G, Sang L, Liu Q, et al. (2019) Effects of dam construction on biodiversity: a review. Journal of Cleaner Production 221:480–489. https://doi.org/10.1016/j.jclepro.2019.03.001

Zabaleta A, Martínez M, Uriarte JA, Antigüedad I (2007) Factors controlling suspended sediment yield during runoff events in small headwater catchments of the Basque Country. Catena 71:179–190. https://doi.org/10.1016/j.catena.2006.06.007

Supporting Information

The following information may be found in the online version of this article:

Table S1. Full output of the results of the linear mixed-effects models of water physicochemical attributes.

Table S2. Full output of the results of the linear mixed-effects models of biofilm structural and functional attributes.

Coordinating Editor: Margaret Palmer

Received: 23 January, 2022; First decision: 16 March, 2022; Revised: 24 August, 2022; Accepted: 26 August, 2022